ISSN 1674-1056
http://cpb.iphy.ac.cn
http://iopscience.iop.org/cpb
中国物理 B
Chinese Physics
中国物理 Chinese Physics B

Dyson-Maleev theory of *X X Z* ferrimagnetic spin chain with single-ion anisotropy

Yu-Ge Chen(陈宇戈), Yin-Xiang Li(李殷翔), Li-Jun Tian(田立君), Bin Chen(陈斌)

Citation: Chin. Phys. B . 2018, 27(12): 127501. **doi:** 10.1088/1674-1056/27/12/127501
Journal homepage: http://cpb.iphy.ac.cn; http://iopscience.iop.org/cpb

What follows is a list of articles you may be interested in

Magnetism induced by Mn atom doping in SnO monolayer

Ruilin Han(韩瑞林), Yu Yan(闫羽)

Chin. Phys. B . 2018, 27(11): 117505. **doi:** 10.1088/1674-1056/27/11/117505

Magnetic properties of AlN monolayer doped with group 1A or 2A nonmagnetic element: First-principles study

Ruilin Han(韩瑞林), Xiaoyang Chen(陈晓阳), Yu Yan(闫羽)

Chin. Phys. B . 2017, 26(9): 097503. **doi:** 10.1088/1674-1056/26/9/097503

Electronic structures and magnetic properties of Zn- and Cd-doped AlN nanosheets: A first-principles study

Rui-Lin Han(韩瑞林), Shi-Min Jiang(姜世民), Yu Yan(闫羽)

Chin. Phys. B . 2017, 26(2): 027502. **doi:** 10.1088/1674-1056/26/2/027502

Schwinger-boson approach to anisotropy ferrimagnetic chain with bond alternation

Li Yin-Xiang, Chen Bin

Chin. Phys. B . 2015, 24(2): 027502. **doi:** 10.1088/1674-1056/24/2/027502

Multiple sign reversals of the exchange bias field in polycrystalline $SmCr_{0.9}Fe_{0.1}O_3$

Fang Yong, Yan Shi-Ming, Gong Yuan-Yuan, Zhu Wei-Li, Cao Qing-Qi, Wang Dun-Hui, Du You-Wei

Chin. Phys. B . 2014, 23(12): 127502. **doi:** 10.1088/1674-1056/23/12/127502

Dyson–Maleev theory of an XXZ ferrimagnetic spin chain with single-ion anisotropy*

Yu-Ge Chen(陈宇戈)[1], Yin-Xiang Li(李殷翔)[2,†], Li-Jun Tian(田立君)[1], and Bin Chen(陈斌)[2,‡]

[1] College of Sciences, Shanghai University, Shanghai 200444, China

[2] Tin Ka-Ping College of Science, University of Shanghai for Science and Technology, Shanghai 200093, China

(Received 28 April 2018; revised manuscript received 18 September 2018; published online 10 November 2018)

We use the mean-field approximation of Dyson–Maleev representation to study an XXZ Heisenberg ferrimagnetic spin chain with single-ion anisotropy. By solving the self-consistent equations with different anisotropies, λ and D respectively, the energy spectrums, internal energy, static susceptibility and specific heat are calculated. Especially, the quantum phase transition of the magnetization plateau induced by single-ion anisotropy D is obtained in the model of the ferrimagnetic spin chain by using Dyson–Maleev mean-field theory.

Keywords: Dyson–Maleev mean-field theory, XXZ anisotropy, Single-ion anisotropy, ferrimagnetic spin chain

PACS: 75.40.Cx, 75.50.Gg **DOI:** 10.1088/1674-1056/27/12/127501

1. Introduction

Since the discovery of high-temperature superconductivity in cuprates,[1] the question of the link between the mechanism of unconventional superconductivity and magnetic order in low-dimensional antiferromagnets is still unanswered for theoretical and experimental researchers. In particular, for one-dimensional system, the interplay between strong quantum fluctuation and competing interaction generates a series of new exotic states, such as spin-Peierls states, magnetic plateau and spin liquid states. Haldane[2] pointed out that the excited spectrum of an integer spin chain is gapped while that of a half-integer spin chain is gapless. This statement pushed experimenters to verify and led to substantial interest in new quasi-one-dimensional magnetic materials. The mixed spin chain, which consists of two different spins, S and s, is one of the active models in low-dimensional magnets. The spin-alternating ferrimagnetic chain materials have been synthesized in the laboratory, such as $NiCu(pba)(D_2O)_3 \cdot D_2O$.[3] From a theoretical point of view, the powerful mean-field methods for dealing with one-dimensional spin model work very well, such as the Schwinger-boson mean-field (SBMF),[4–6] the Dyson–Maleev mean-field (DMMF),[7–11] the modified spin wave (MSW),[12] and the bond operator (BO).[13–18] Besides the above mean-field methods, various numerical methods have been applied to study the field of low-dimensional magnets, such as QMC,[19] DMRG,[12] and ED.[12] For low-dimension magnets, the quantization of magnetization, a plateau in magnetization curve, is an interesting phenomenon. Such plateaux have been found in real materials such as bond-alternating chains,[20] the Shastry–Sutherland system $SrCu_2(BO_3)_2$,[21–23] the zigzag double chain NH_4CuCl_3,[24] and the frustrated spin ladder.[25] The ferrimagnetic spin chain has spontaneous magnetization $m = S - s$ in the ground state. In some real materials, the longitudinal spin interaction is different; it has a transverse term which means that the spin can be locked in one direction in the limitation. Another phenomenon has been observed that the anisotropy in spin-1 Ni^{2+} ions is much larger than that in spin-1/2 Cu^{2+}-ions, which is caused by the spin–orbit effect in the spin space. Sakai[26] observed the quantum phase transition of magnetization in the ferrimagnetic spin chain by numerical exact diagonalization. In this paper, we use the Dyson–Maleev mean-field approximation to deal with the model of an XXZ Heisenberg spin ferrimagnetic chain with single-ion anisotropy.

The paper is organized as follows. In the second section, we present the Dyson–Maleev mean-field approximation for an XXZ ferrimagnetic spin chain with single-ion anisotropy. In the third section, we obtain the excited spectrums at zero temperature and numerical results of internal energy, magnetization plateau, static susceptibility, and specific heat at finite temperature based on the effect of single-ion anisotropy D. In the forth section, we discuss the ferrimagnetic spin chain model with XXZ anisotropy λ. Subsequently, we also discuss the corresponding numerical results of energy spectrums, internal energy, static susceptibility, and specific heat. A sum-

*Project supported by the National Natural Science Foundation of China (Grant No. 10774035) and the Qianjiang RenCai Program of Zhejiang Province, China (Grant No. 2007R0010).

†Corresponding author. E-mail: yinxiangl@hotmail.com

‡Corresponding author. E-mail: chenbin@usst.edu.cn

© 2018 Chinese Physical Society and IOP Publishing Ltd

mary is made in the final section.

2. Dyson–Maleev representation for spin-1/2 and spin-1 *XXZ* ferrimagnetic chain with single-ion anisotropy

In real bulk crystals, the longitudinal magnetic interaction is different with transverse coupling, which is related to the model of XXZ anisotropy. Due to spin–orbit coupling, the anisotropy effect in a spin-1/2 ion is much weaker than that in a spin-1 ion. Thus, we only consider the anisotropy of spin-1 ions, namely single-ion anisotropy, in the Heisenberg ferrimagnetic spin chain model. In the following, we mainly discuss these two types of anisotropic effects in the ferrimagnetic spin chain model. The Hamiltonian of spin-1/2 and spin-1 XXZ ferrimagnetic spin chains with single-ion anisotropy under external magnetic field h is

$$\begin{aligned} H = &\frac{1}{2}\sum_{ij}(s_i^+ s_j^- + s_i^- s_j^+) + \lambda\sum_{ij} s_i^z s_j^z \\ &- D\sum_j (s_j^z)^2 + \sum_i h s_i^z + \sum_j h s_j^z, \end{aligned} \tag{1}$$

where $s^{\pm}_{i(j)} = s^x_{i(j)} \pm \mathrm{i}s^y_{i(j)}$, $s_i = 1/2$ and $s_j = 1$. λ is the XXZ anisotropic parameter and D is the single-ion anisotropic parameter. Compared with the Holstein–Primakoff transformation,[27] unphysical states in the truncation of asymptotic square-root series are deleted in the Dyson–Maleev formalism. For ferrimagnetic spin chain, the Dyson–Maleev representation of spin operators can be shown as follows:

$$\begin{aligned} &s_i^+ = (2s_1)^{-1/2}(2s_1 a_i - a_i^\dagger a_i a_i), \quad s_i^- = (2s_1)^{1/2} a_i^\dagger, \\ &s_i^z = s_1 - a_i^\dagger a_i, \quad s_j^+ = (2s_2)^{-1/2}(2s_2 b_j^\dagger - b_j^\dagger b_j^+ b_j), \\ &s_j^- = (2s_2)^{1/2} b_j, \quad s_j^z = -s_2 + b_j^\dagger b_j, \end{aligned} \tag{2}$$

where $s_1 = s_i = 1/2$ and $s_2 = s_j = 1$. The operators a_i and b_j, which are defined on the lattice sites $i \in A$ and $j \in B$ respectively, satisfy the bosonic communication relation

$$[a_i, a_i^\dagger] = 1, \ \ [b_j, b_j^\dagger] = 1, \ \ [a_i, b_j] = 0, \ \ [a_i^\dagger, b_j^\dagger] = 0. \tag{3}$$

By substituting the above boson operators into formula (1), the Hamiltonian can be rewritten as

$$\begin{aligned} H = &\frac{1}{2}\sum_{ij}\left[\sqrt{2}(a_i b_j - a_i^\dagger a_i a_i b_j) + \frac{\sqrt{2}}{2}(2a_i^\dagger b_j^\dagger - a_i^\dagger b_j^\dagger b_j^\dagger b_j)\right] \\ &+ \lambda\sum_{ij}\left(-\frac{1}{2} + \frac{1}{2}b_j^\dagger b_j + a_i^\dagger a_i - a_i^\dagger a_i b_j^\dagger b_j\right) \\ &- D\sum_j (b_j^\dagger b_j b_j^\dagger b_j - 2b_j^\dagger b_j + 1) \\ &- h\sum_i a_i^\dagger a_i + h\sum_j b_j^\dagger b_j - \frac{1}{2}h. \end{aligned} \tag{4}$$

In the mean-field approximation, we assume that $\langle a_i^\dagger a_i\rangle = P$, $\langle b_j^\dagger b_j\rangle = Q$, and $\langle a_i^\dagger b_j^\dagger\rangle = \langle a_i b_j\rangle = M$. Those four-operator interaction terms can be decoupled as

$$\begin{aligned} &a_i^\dagger a_i a_i b_j = \langle a_i^\dagger a_i\rangle a_i b_j + a_i^\dagger a_i \langle a_i b_j\rangle - \langle a_i^\dagger a_i\rangle\langle a_i b_j\rangle, \\ &a_i^\dagger b_j^\dagger b_j^\dagger b_j = \langle a_i^\dagger b_j^\dagger\rangle b_j^\dagger b_j + a_i^\dagger b_j^\dagger \langle b_j^\dagger b_j\rangle - \langle a_i^\dagger b_j^\dagger\rangle\langle b_j^\dagger b_j\rangle, \\ &a_i^\dagger a_i b_j^\dagger b_j = \langle a_i^\dagger b_j^\dagger\rangle a_i b_j + a_i^\dagger b_j^\dagger \langle a_i b_j\rangle - \langle a_i^\dagger b_j^\dagger\rangle\langle a_i b_j\rangle. \end{aligned} \tag{5}$$

In the moment space, the Hamiltonian can be obtained as

$$\begin{aligned} H = &\psi^+ W\psi + \frac{\sqrt{2}}{2}zPM + \frac{\sqrt{2}}{4}zQM - \frac{1}{2}z\lambda + M^2 z\lambda \\ &- \left(-\frac{\sqrt{2}}{4}M + \frac{1}{2}\lambda\right)z + 2D(Q-1)z \\ &+ zDQ^2 - Dz - \frac{3}{2}h, \end{aligned} \tag{6}$$

where

$$\begin{aligned} &W = \begin{pmatrix} a & b \\ c & d \end{pmatrix}, \quad \psi = \begin{pmatrix} a_k \\ b_k^+ \end{pmatrix}, \\ &a = \left(-\frac{\sqrt{2}}{2}M + \lambda\right)z - h, \\ &b = \left[\frac{\sqrt{2}}{4}(2-Q) - M\lambda\right]z\gamma_k, \\ &c = \left[\frac{\sqrt{2}}{2}(1-P) - M\lambda\right]z\gamma_k, \\ &d = \left(-\frac{\sqrt{2}}{4}M + \frac{1}{2}\lambda\right)z - 2D(Q-1)z + h, \end{aligned}$$

$z = 2$ is the number of the nearest neighbors and $\gamma_k = \cos(k)$. The energy spectrums are

$$\begin{aligned} E^+ &= \frac{1}{2}\left[(a-d) + \sqrt{(a+d)^2 - 4bc}\right], \\ E^- &= \frac{1}{2}\left[-(a-d) + \sqrt{(a+d)^2 - 4bc}\right]. \end{aligned} \tag{7}$$

To obtain the parameters P, Q, and M, we solve the self-consistent equations numerically by

$$\frac{\partial H}{\partial P} = \frac{\partial H}{\partial Q} = \frac{\partial H}{\partial M} = 0$$

as follows:

$$\frac{\sqrt{2}}{2}zM = -\frac{1}{4N}\sum\left(\coth\left(\frac{E^+}{2T}\right) + \coth\left(\frac{E^-}{2T}\right)\right)\frac{\left(\sqrt{2}/2\right)\left[\left(\sqrt{2}/4\right)(2-Q) - M\lambda\right]z^2\gamma_k^2}{\sqrt{(a+d)^2 - 4bc}}, \tag{8}$$

$$\frac{\sqrt{2}}{4}zM+2Dz+2zDQ=-\frac{1}{4N}\sum\left\{\left(\coth\left(\frac{E^+}{2T}\right)-\coth\left(\frac{E^-}{2T}\right)\right)2D \tag{9}$$

$$+\left(\coth\left(\frac{E^+}{2T}\right)+\coth\left(\frac{E^-}{2T}\right)\right)\frac{-2D(a+d)+(\sqrt{2}/4)\left[(\sqrt{2}/2)(1-P)-M\lambda\right]z^2\gamma_k^2}{\sqrt{(a+d)^2-4bc}}\Bigg\}, \tag{10}$$

$$\frac{\sqrt{2}}{2}zP+\frac{\sqrt{2}}{4}zQ+2Mz\lambda+\frac{\sqrt{2}}{4}z=-\frac{1}{4N}\sum\left\{\left(-\coth\left(\frac{E^+}{2T}\right)+\coth\left(\frac{E^-}{2T}\right)\right)\frac{\sqrt{2}}{4}+\left(\coth\left(\frac{E^+}{2T}\right)+\coth\left(\frac{E^-}{2T}\right)\right)\right. \tag{11}$$

$$\left.\cdot\frac{-(3\sqrt{2}/4)(a+d)+\lambda\left[\left((\sqrt{2}/2)(1-P)-M\lambda\right)+\left((\sqrt{2}/4)(2-Q)-M\lambda\right)\right]z^2\gamma_k^2}{\sqrt{(a+d)^2-4bc}}\right\}. \tag{12}$$

In the subsequent sections, we only consider different anisotropic effects D and λ separately in the ferrimagnetic spin model. The competition between XXZ anisotropy and single-ion anisotropy is neglected in this paper.

3. Numerical results with single-ion anisotropy D at the Heisenberg point

In this part, we only consider the effect of single-ion anisotropy D on a ferrimagnetic spin chain at the Heisenberg point ($\lambda = 1$) without XXZ anisotropy. We obtain two branches of excitation spectrums, as shown in Fig. 1, by numerically solving the above self-consistent equations with different parameters D at zero temperature. When anisotropic parameter D equals 0, the energy spectrums of system have a gapful branch and a nearly gapless branch. When anisotropy is increased, these two energy branches have distinct trends. The lower branch increases comparatively faster than the other branch. With the increasing of anisotropic parameter, the energy spectrums become two gapful branches and the bandwidth of energy spectrums is narrower.

For a low-dimensional magnetic system, the quantum phase transition of the magnetization plateau is a prevalent and exotic phenomenon in spin-alternating chains and ladders. According to the generalized Lieb–Schulz–Mattis theorem,[28] the system may have a nontrivial magnetization plateau at $m = 0.5$ in spin-(1/2,1) ferrimagnetic chain. We assume that the uniform magnetic field is imposed along the Z direction of $s_j = 1$. The magnetization under external magnetic field is shown in Fig. 2. Due to the increase of the energy gap of the lower excitation spectrum with bigger anisotropy, the trivial plateau at $m = 0$ becomes longer, which means that system needs a sufficiently stronger external magnetic field to close the gap. When the magnetic field is enhanced further, the system stays in the nontrivial phase $m = 0.5$ up to the saturation field. This quantum nontrivial plateau of magnetization disappears at the critical point $D_c = 0.127$. This quantum phase transition is caused by the energy gap between two branches, and it is closed with larger single-ion anisotropy D. When the anisotropy parameter $D = 0.15$ exceeds the critical value D_c, two cusp singularities have been observed in this system. The existence of a magnetization cusp singularity due to the dispersion of magnon excitations has a minimum at an incommensurate wave vector value.[29] Compared with other methods for the critical point of magnetization plateau, our mean-field result is larger than classical spin system ($D_c = 0.057$) and is smaller than the exact diagonalization calculation ($D_c = 1.1$) in Sakai's paper.[26] The value of the critical point is sensitive for different methods. We calculate T times uniform static susceptibility per unit site $T\chi_{uni}/Ng^2$ versus temperature with a small magnetic field as shown in Fig. 3. The uniform susceptibility increases with the increase of temperature. The susceptibility with smaller anisotropic parameter D is bigger than that with larger D. Figure 4 shows the variation of magnon internal energy at finite temperature. The internal energy becomes smaller with continually adding anisotropic parameter D. When the temperature increases, it is well known that the system will have more energy. The temperature dependence of specific heat with different parameters D is plotted in Fig. 5. It is found that the specific heat increases linearly in the temperature region $[0.2, 0.5]$. The line with larger parameter D is enhanced more rapidly. Thus, there are some crossing points in this region.

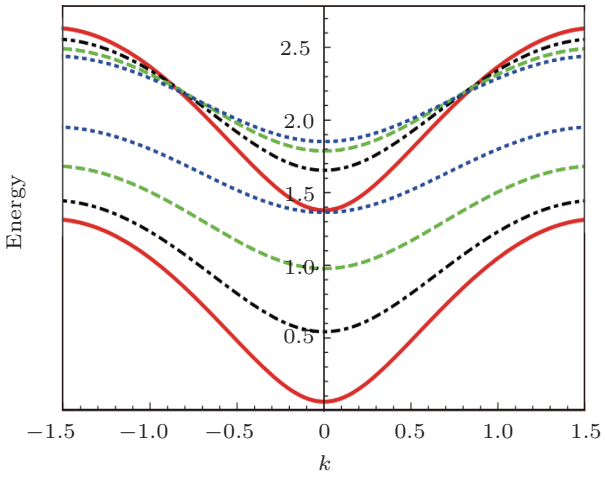


Fig. 1. (color online) Energy spectrums with different single-ion anisotropic parameters $D = 0$ (red solid), $D = 0.05$ (black dot–dashed), $D = 0.1$ (green dashed) and $D = 0.15$ (blue dotted) at zero temperature.

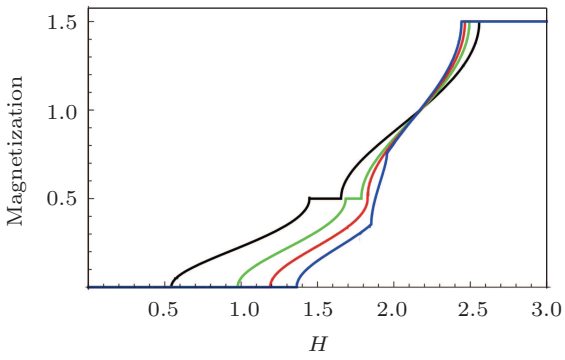


Fig. 2. (color online) Magnetization plateau with different parameters $D = 0.05$ (black), $D = 0.1$ (green), $D = 0.127$ (red), and $D = 0.15$ (blue) under an uniform magnetic field H at zero temperature.

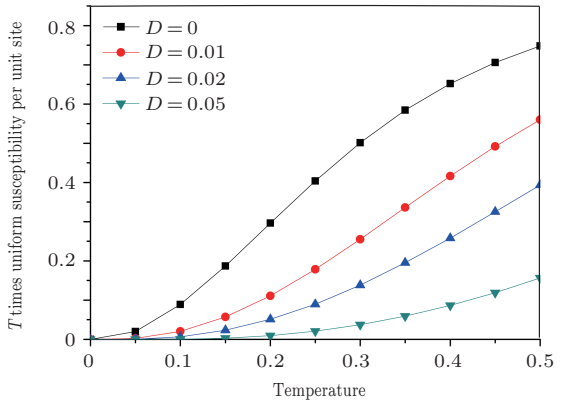


Fig. 3. (color online) Static susceptibility with different parameters D at finite temperature.

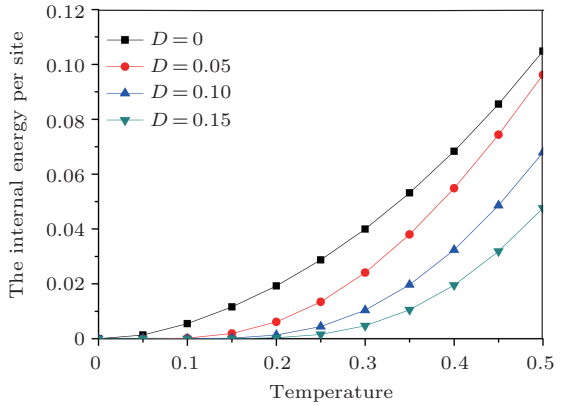


Fig. 4. (color online) Magnon internal energy with different parameters D at finite temperature.

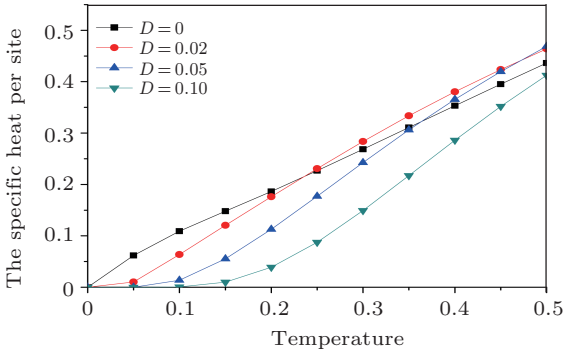


Fig. 5. (color online) Specific heat with different parameters D at finite temperature.

4. Numerical results with *XXZ* anisotropy λ

In this part, we discuss the effect of XXZ anisotropy by solving the self-consistent equations with anisotropic parameter λ. With the increase of the XXZ parameter λ, two excitation spectrums are lifted gradually and the lower branch has a larger gap, as shown in Fig. 6. Compared with the single-ion anisotropy effect, the bandwidth with XXZ anisotropy does not change significantly. Figure 7 shows the variation of internal energy depending on XXZ anisotropy. The magnon internal energy can be calculated by the formula

$$U(T) = \sum_k \left(\frac{E_k^+}{\exp[E_k^+/T] - 1} + \frac{E_k^-}{\exp[E_k^-/T] - 1} \right).$$

The energy with larger XXZ anisotropy is continually decreasing. This trend of internal energy is similar to the effect of single-ion anisotropy.

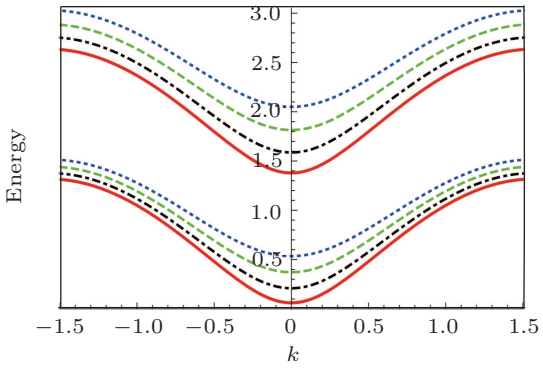


Fig. 6. (color online) Energy spectrums with different XXZ anisotropic parameters $\lambda = 1.0$ (red solid), $\lambda = 1.1$ (black dotdashed), $\lambda = 1.2$ (green dashed) and $\lambda = 1.3$ (blue dotted) at zero temperature.

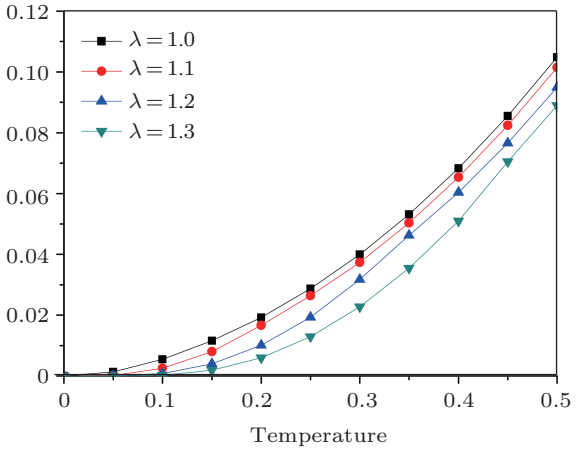


Fig. 7. (color online) Internal energy with different parameters λ at finite temperature.

Under a small external magnetic field, T times uniform static susceptibility per unit site $T\chi_{\text{uni}}/Ng^2$ versus temperature is calculated, as shown in Fig. 8. Compared with the curve, $\lambda = 1.0$ is an increasing linear function, the curve $\lambda = 1.3$ is nearly a power law. When the parameter λ is added from 1.0 to 1.3, the trend of static susceptibility is similar to the

combination of the above two curves. The susceptibility with larger anisotropy becomes smaller at low temperature. It is undoubtable that the effect of XXZ anisotropy on static susceptibility is apparent.

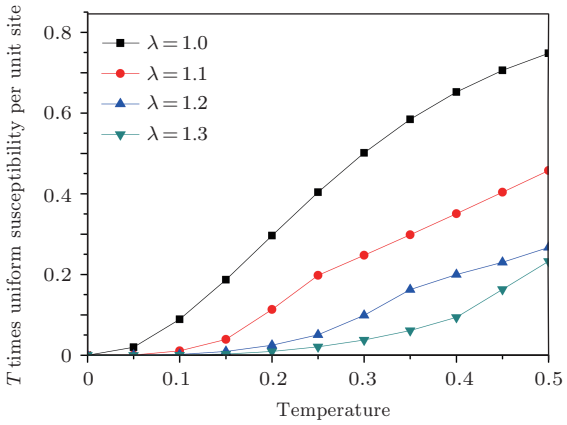


Fig. 8. (color online) Static susceptibility with different parameters λ at finite temperature.

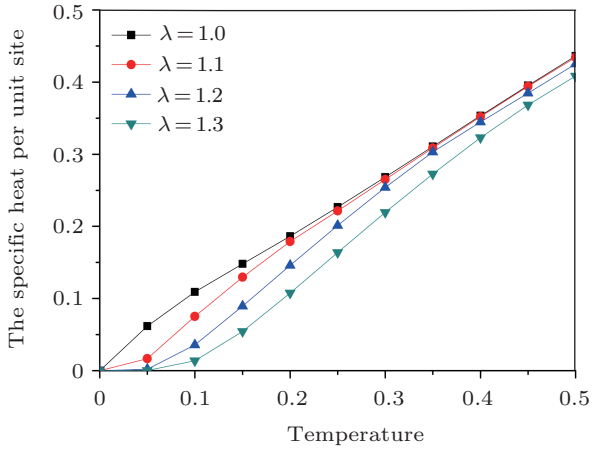


Fig. 9. (color online) Specific heat with different parameters λ at finite temperature.

Figure 9 shows the specific heat with different XXZ anisotropy, which is calculated by the numerical differentiation of the internal energy U with T. As shown in the figure, the effect of XXZ anisotropy is not definitely different with single-ion anisotropy. The curve with anisotropy λ is enhanced slowly at first and then becomes linear. The specific heat is calculated from the differentiation of magnon internal energy. Thus, the numerical number of specific heat has the same behavior as internal energy, which is smaller with larger anisotropy.

5. Summary

Based on the method of Dyson—Maleev mean-field approximation, we discuss two types of anisotropic effects, XXZ anisotropy and single-ion anisotropy, in the Heisenberg spin ferrimagnetic chain model. With different XXZ anisotropic parameter λ and single-ion anisotropic parameter D, we obtain the energy spectrums, internal energy, static susceptibility, and specific heat separately. The quantum phase transition of the magnetization plateau, which is caused by the single-ion anisotropy, is also observed in our Dyson–Maleev mean-field calculation. The magnetization plateau phenomenon is ubiquitous in the mixed spin system.

References

[1] Bednorz J G and Muller K A 1986 *Physica B* **64** 189
[2] Haldane F D M 1983 *Phys. Rev. Lett.* **50** 1153
[3] Hagiwara M, Minami K, Narumi Y, Tatani K and Kindo K 1998 *J. Phys. Soc. Jpn.* **67** 2209
[4] Wu C J, Chen B, Dai X, Yu L and Su Z B 1999 *Phys. Rev. B* **60** 1057
[5] Li Y X and Chen B 2010 *Phys. Lett. A* **374** 3514
[6] Li Y X and Chen B 2015 *Chin. Phys. B* **24** 027502
[7] Dyson F 1956 *Phys. Rev.* **102** 1217
[8] Dyson F 1956 *Phys. Rev.* **102** 1230
[9] Maleev S V 1958 *Sov. Phys. JETP* **6** 776
[10] Albuquerque A F, Pires A S T and Gouvea M E 2005 *Phys. Rev. B* **72** 174423
[11] Chen Y G, Li Y X, Tian L J and Chen B 2017 *Phys. Lett. A* **381** 2872
[12] Yamamoto S, Fukui T, Maisinger K and Schll?ck U 1998 *J. Phys.: Condens. Matter* **10** 11033
[13] Sachdev S and Bhatt R N 1990 *Phys. Rev. B* **41** 9323
[14] Wang H T, Shen J L and Su Z B 1997 *Phys. Rev. B* **56** 14435
[15] Wang H T, Lin H Q and Shen J L 2000 *Phys. Rev. B* **61** 4019
[16] Kumar B 2010 *Phys. Rev. B* **82** 054404
[17] Li Y X and Chen B 2015 *Phys. Lett. A* **379** 408
[18] Chen Y G, Li Y X, Tian L J and Chen B 2017 *Physica B* **520** 65
[19] Brehmer S, Mikeska H J and Yamamoto S 1997 *J. Phys.: Condens. Matter* **9** 3921
[20] Hagiwara M, Kobayashi K and Chihara T 1997 *J. Phys. Soc. Jpn.* **66** 1702
[21] Miyahara S and Ueda K 1999 *Phys. Rev. Lett.* **82** 3701
[22] Qin M H, Zhang G Q, Wang K F, Gao X S and Liu J M 2011 *J. Appl. Phys.* **109** 07E103
[23] Hou L, Huang W C, Yan Z B, Jia X T, Gao X S, Qin M H and Liu J M 2013 *J. Appl. Phys.* **113** 073908
[24] Kolezhuk A K 1999 *Phys. Rev. B* **59** 4181
[25] Tandon K, Lal S, Pati S K, Ramasesha S and Sen D 1999 *Phys. Rev. B* **59** 396
[26] Sakai T and Okamoto K 2002 *Phys. Rev. B* **65** 392
[27] Holstein T and Primakoff H 1940 *Phys. Rev.* **58** 1098
[28] Oshikawa M, Yamanaka M and Affleck I 1997 *Phys. Rev. Lett.* **7** 1984
[29] Okunishi K, Hieida Y and Akutsu Y 1999 *Phys. Rev. B* **60** R6953